A Study by Spectroelectrochemical FTIR and Density Functional Theory Calculations of the Reversible Complexing Ability of an Electroactive Tetrathiafulvalene Crown

C. Wartelle,[†] P. M. Viruela,[‡] R. Viruela,[‡] E. Ortí,[‡] F. X. Sauvage,*[,†] E. Levillain,[§] F. Le Derf,[§] and M. Sallé[§]

LASIR-HEI, UMR CNRS 8516, 13 rue de Toul, F-59046 Lille Cedex, France, Departament de Química Física, Institut de Ciència Molecular, Universitat de València, Dr. Moliner 50, E-46100 Burjassot (València), Spain, and Groupe Systèmes Conjugués Linéaires, CIMMA, UMR CNRS 6200, 2 Bd Lavoisier, F-49045 Angers Cedex, France

Received: October 8, 2004; In Final Form: November 16, 2004

We report on the study of the electrochemically targeted complexation/expulsion of a metal cation (Ba^{2+}) by a crown ether tetra(thiomethyl)tetrathiafulvalene derivative (crown-TTM-TTF). Real time, in situ FTIR spectroelectrochemistry was used to obtain spectroscopic evidence of this electrochemically triggered phenomenon. Density functional theory calculations allowed the spectral information collected to be assigned. Both experimental and theoretical results clearly show that neutral crown-TTM-TTF complexes well Ba^{2+}. Complexation is evidenced by a significant downshift of the frequency corresponding to the asymmetric stretching of the C−O−C ether groups. Concerning the cation crown-TTM-TTF, the spectroscopic signal of the complex form was difficult to identify, first because of the rather low value of the complexation constant and second because the vibration modes involving the oxygen atoms (which are the most affected by the complexation) were found by calculation to occur in the lower spectral region (<1000 cm^{-1}), which is not accessible in our experimental conditions. In the case of the dication crown-TTM-TTF, it is now clear that the complex form does not exist, which means that the electrochemical formation of the dication necessarily involves the expulsion of the barium ion.

1. Introduction

The discovery of crown ethers by Pedersen in 1962 opened new possibilities for complexing metal cations.[1] In particular, much effort has been dedicated to develop molecular assemblies incorporating these receptors with the additional possibility of controlling the complexation process: molecular systems made up of a macrocyclic receiver combined with an electroactive unit. Among redox-active compounds, tetrathiafulvalene (TTF) has emerged as an alternative electroactive system in the design of redox-responsive ligands. TTF and its derivatives have been widely investigated,[2] and have been the focus of a great number of studies in the field of materials chemistry.[3] TTF derivatives are versatile building blocks that are used in the preparation of cation sensors, liquid crystals, shuttles and switches, redox polymers, photovoltaic materials, etc.[4] Most of these applications are related to the redox properties of TTF. It is an excellent π-electron donor and can be successively oxidized into thermodynamically stable radical cation and dication species, in a totally reversible way.

The synthesis of crown ether derivatives incorporating the TTF unit has been exploited with the aim of creating compounds that would be able to complex metal cations and so that this complexation could be monitored electrochemically. To ensure a good communication between the chelating unit (the crown ether) and the redox moiety (the TTF core), the functionalization of the TTF moiety has been undertaken following different strategies of synthesis.[3a,c,d,e,5] In a recent study, the synthesis and properties of the crown ether derivative of tetra(thiomethyl)-tetrathiafulvalene (TTM-TTF) displayed in Figure 1 have been described.[6] This molecule (hereafter referred to as "crown-TTM-TTF") is able to complex the barium metal cation. The electrochemical study performed by cyclic voltammetry (CV) revealed that the molecule keeps the redox properties of TTF; i.e., it oxidizes in two successive, fully reversible steps ($E_{OX}^1 = 0.53$ V and $E_{OX}^2 = 0.73$ V vs Ag/AgCl).[6a] The complexation with the barium cation affects the electrochemical behavior. Progressive additions of barium perchlorate cause an anodic shift of 100 mV of the first oxidation wave (E_{OX}^1), while the second oxidation wave (E_{OX}^2) remains unchanged. The anodic shift of E_{OX}^1 is taken as the electrochemical signature of the complexation of Ba^{2+} by crown-TTM-TTF, and it is attributed to an inductive electrostatic effect of the crown ether bound metal cation, which determines a decrease of the electronic density on the TTF moiety. On the other hand, the second oxidation wave is neither shifted nor modified, which seems to indicate that, at this point, crown-TTM-TTF is in its "free" (not complexed) dication form. The repulsive electrostatic interaction

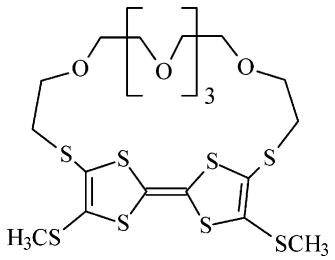

Figure 1. Chemical structure of crown-TTM-TTF.

* To whom correspondence should be addressed. Phone: +333 28 38 48 58. Fax: +333 28 38 48 04. E-mail: fxsauvage@hei.fr.
[†] UMR CNRS 8516.
[‡] Universitat de València.
[§] UMR CNRS 6200.

10.1021/jp045397y CCC: $30.25
Published on Web 01/20/2005

caused by the double positive charge has already expelled the metal cation from the cage. The CV values of the complexation constants obtained for the crown-TTM-TTF/barium system were $K^0 = 1.9 \times 10^4$ for the neutral state, $K^+ = 2.4 \times 10^2$ for the radical cation, and $K^{2+} \approx 0$ for the dication.[6]

In this paper, we aim to provide a spectroscopic signature of the complexing ability of crown-TTM-TTF by using in situ, real time vibration spectroelectrochemistry. This technique allows the potential to be controlled, while returning salient structural information about the species formed during the experiment through the observation of the absorption frequencies.[7] The technique was developed by Gaillard et al., who worked out a cell suited for both UV−vis and Raman spectroscopy.[8] The applicability of this cell was recently extended to IR[9] and fluorescence.[10] To get a deeper understanding of the experimental observations, the spectroelectrochemistry study was complemented with density functional theory (DFT) calculations. In a recent study on TTF and TTM-TTF,[11] this approach has been shown to be a powerful tool in interpreting the experimental trends obtained from FTIR spectroelectrochemistry.

2. Experimental and Computational Details

Spectroelectrochemical Measurements. The spectroelectrochemical cell has been described elsewhere, and its operational ability was checked with the well-known, two-step reduction of tetracyano-*p*-quinodimethane (TCNQ).[9] The optical window used for FTIR measurements is CaF_2, which is IR-transparent down to ca. 1111 cm^{-1}, although it is possible to observe IR signals down to ca. 1000 cm^{-1}. Because of the energy attenuation in the range 1100−1000 cm^{-1}, the signals observed in this range have to be taken into account with due care.

Spectroelectrochemical measurements were carried out with a Bruker Tensor 27 FTIR instrument equipped with an MCT detector cooled with liquid nitrogen. This spectrometer allows collection of two spectra per second. The electrochemical (cyclic voltammetry) part of the experiment was run with an Autolab PGSTAT 100 potentiostat. Measurements were carried out in thin layer conditions to ensure total electrolysis conditions of the probed sample, which implies low scan rates (1−5 $mV \cdot s^{-1}$), and to keep the absorption of the IR peaks below a value of ca. 0.8. In all cases, a compromise had to be found, and typically, the thickness of the layer (i.e., the optical path) was kept below 100 μm. We always managed to collect about 100 infrared spectra along the electrochemical scanning range (0−1 V and back), i.e., over the total duration of the experiment.

The series of spectra collected contained rather complex information: strong signals due to both the solvent and the supporting electrolyte and much weaker signals due to the solute (crown-TTM-TTF). Accordingly, considering the remarkable stability of the infrared spectrometer and to evidence the changes undergone upon oxidation, the first spectrum recorded at the starting potential (0.0 V) was systematically subtracted from all the others. All the resulting "difference spectra" were then assembled in a 3D plot (variation of absorbance/applied potential/wavenumber) called a "difference spectroelectrogram". The data are raw and have been neither corrected nor smoothed, which further demonstrates the excellent quality of the experimental setup and signal-to-noise ratio.

The solutions studied were 10^{-3} M in crown-TTM-TTF in acetonitrile/dichloromethane (50:50 mixture, Merck, spectroscopic grade), containing 0.1 M tetrabutylammonium hexafluorophosphate ($TBAPF_6$; supporting electrolyte, Fluka). The equimolar mixture of solvents was chosen because the metal cation is soluble in CH_2Cl_2 and the crown ether is better dissolved in CH_3CN. These rather harsh conditions were necessary because a higher concentration of crown ether can cause the formation of aggregates.[12]

The working electrode was a 5 mm platinum disk, and the reference electrode was Ag^+/Ag in $CH_3CN-TBAPF_6$. The counter electrode was a broad piece of platinum foil. All solutions were prepared and the cell was filled in a glovebox flushed with dry (H_2O contents <0.1 vpm), deoxygenated argon (O_2 contents <0.1 vpm).

Computational Details. DFT calculations were carried out using the GAUSSIAN 03 program package[13] running on SGI Altix computers and IBM RS/6000 workstations. All calculations were performed using Becke's three-parameter B3P86 exchange-correlation functional,[14] together with the 6-31G** basis set.[15] The B3P86 functional is recognized to provide equilibrium geometries for sulfur-containing compounds in better agreement with experimental data and ab initio post-Hartree−Fock (HF) calculations than the more widely used B3LYP functional.[16] The 6-31G** basis set was chosen as a compromise between accuracy in predicting molecular geometries and computational cost. Geometry-optimization calculations were very expensive in computing time due to the high flexibility of the polyether chain. Calculations without symmetry restrictions took more than 100 optimization cycles to achieve convergence criteria. The LANL2DZ basis set,[17] which incorporates quasirelativistic effective core potentials (ECPs), was used for the Ba atom. The radical cations of both metal-free and Ba^{2+}-complexed systems were treated as open-shell systems and were computed by using spin-unrestricted DFT wave functions (UB3P86). No significant spin contamination was obtained for these systems.

The calculated harmonic vibrational frequencies were scaled down uniformly by a factor of 0.96, as suggested by Scott and Radom.[18] Accordingly, all theoretical vibration data quoted in the text are scaled values. The theoretical infrared spectra were obtained by convoluting the scaled frequencies with Gaussian functions (10 cm^{-1} half-width). The height of the Gaussians was determined from the intensities calculated for the infrared-active normal modes.

3. Results and Discussion

IR Spectroelectrochemistry. *Free Crown-TTM-TTF.* The difference spectroelectrogram obtained for free crown-TTM-TTF is presented in Figure 2. Only the part of the spectral range where a signal was recorded (1600−1000 cm^{-1}) is displayed. It should be noted that in the range 1600−1420 cm^{-1} the solvent used (CH_3CN/CH_2Cl_2, 50:50) absorbs strongly. Consequently, the difference spectrum affords relevant information only in the range 1420−1000 cm^{-1}. The solvent also displays strong absorption bands at 1037, 1265, and 1375 cm^{-1}. Overall, as is always the case in "normal" spectroscopic experiments, salient information will only be available within the solvent's "windows", in our case 1260−1050, 1370−1270, and 1420−1380 cm^{-1}. In Figure 2, the absorption peaks assigned to the solvent are marked with an asterisk and the peaks corresponding to the disappearance ($\Delta A < 0$) of the neutral species and to the formation ($\Delta A > 0$) of the cation and dication are clearly identifiable. It should be stressed that the maximum variation of absorbance is lower than 0.02, which is weaker than what was obtained for TTM-TTF (0.06) in identical conditions.[11] This shows that the experimental setup used is of good quality and yields a good signal-to-noise ratio.

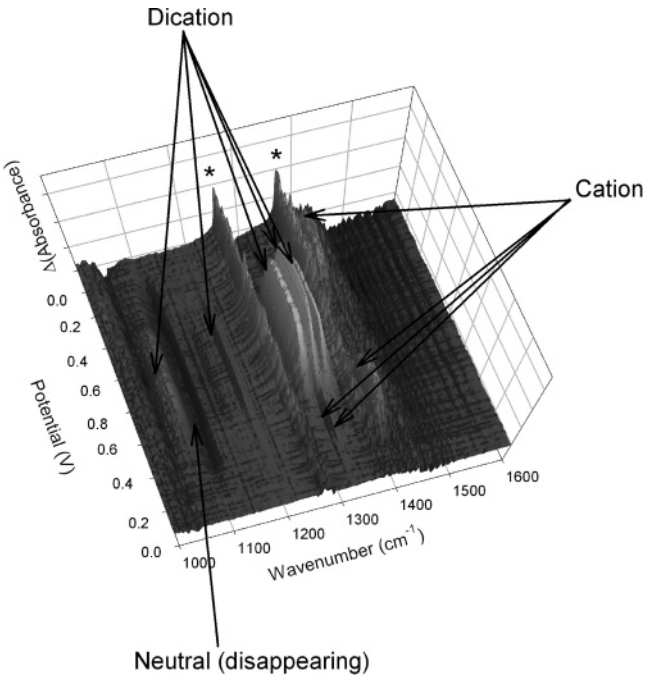

Figure 2. Difference FTIR spectroelectrogram of free crown-TTM-TTF (10^{-3} M) under thin layer conditions in 0.1 M $TBAPF_6$−(CH_3CN/CH_2Cl_2, 50:50). The asterisk denotes absorption peaks of the solvent.

TABLE 1: FTIR Wavenumbers (cm^{-1}) Measured for TTF, TTM-TTF, and Free Crown-TTM-TTF upon Oxidation

	TTF[a]	TTM-TTF[a]	free crown-TTM-TTF
neurtal			1103
		none	
	1530		
cation		1319	1322
		1402	1398
	1477		
	1508		
dication		1091	1074
			1195
		1294	1295
		1310	1315
		1334	1332
	1435		

[a] Values from ref 11.

The wavenumbers of the absorption peaks observed for the different redox species of crown-TTM-TTF are listed in Table 1. The values previously obtained for TTF and TTM-TTF are also included to compare their spectroelectrochemical behavior. A negative peak, necessarily corresponding to the disappearance of the neutral species, is located at 1103 cm^{-1}. The formation of the radical cation determines the appearance of two well-resolved peaks at 1322 and 1398 cm^{-1}. The dication presents two small features at 1074 and 1195 cm^{-1} and an intense band composed of three peaks at 1295, 1315, and 1332 cm^{-1}.

The IR spectroelectrochemical behavior observed for crown-TTM-TTF therefore appears to be very close to that recorded for the TTM-TTF molecule.[11] As observed in Table 1, the number of peaks and their wavenumbers are about the same for both systems. This suggests that grafting a polyetheroxide chain onto TTM-TTF does not disturb too much the molecular structure of that moiety. The spectroelectrochemical differences observed between TTF and TTM-TTF were much more important: the addition of thiomethyl groups to the TTF core involved drastic changes in the resulting spectra.[11]

TABLE 2: FTIR Wavenumbers (cm^{-1}) Measured for Crown-TTM-TTF in Its Neutral, Cation, and Dication States upon Addition of Different Amounts of Barium

	0 equiv	12 equiv	16 equiv	50 equiv
neutral		1079	1079	1079
	1103	1103	1103	1103
cation	1322	1322	1322	1322
			1345 (w)	1345 (w)
	1398	1400	1400	1400
dication	1074			
	1195	1195	1195	1195
	1295	1295	1295	1295
	1315	1315	1315	1315
	1332	1332	1332	1332

Barium Complex of Crown-TTM-TTF. FTIR spectroelectrochemistry measurements were carried out on a solution of crown-TTM-TTF prepared in the same conditions and containing increasing amounts of barium perchlorate. Due to the small crown ether concentration used and to the values of the complexation constants recorded for crown-TTM-TTF and its oxidized species, a barium concentration range of 0−50 equiv had to be covered to obtain a concentration of complexed species compatible with spectroscopic detection. The electrochemical behavior of crown-TTM-TTF upon addition of barium reproduces what was described before.[6]

The wavenumbers recorded for the neutral, radical cation, and dication absorbing species are listed in Table 2 for different amounts of barium added (0, 12, 16, and 50 equiv). Compared to that of the free molecule, the negative peak corresponding to the neutral species is downshifted by 24 cm^{-1} (from 1103 to 1079 cm^{-1}). Indeed, it is rather remarkable to observe this shift for the first additions of barium (<12 equiv), considering that the peak of the complexed neutral species (1079 cm^{-1}, negative peak) and that of the dication (1074 cm^{-1}, positive peak) are located very close to each other. Moreover, the peaks located in this region have an absorbance smaller than 0.01.

For the radical cation, a small peak ($A \approx 0.001$) appears systematically at 1345 cm^{-1}, starting from 16 equiv. Since the complexation constant is 100 times lower than that of the neutral species, a large excess of barium should be added to the solution to be able to observe spectroscopically the complexed cation. From 16 equiv, an appreciable part of the crown-TTM-TTF radical cation is complexed with barium (7.8×10^{-4} M) and the signals of both the metal-free and the complexed radical cation can be observed.

As for the dication, even with 50 equiv of barium added, no spectroscopic difference is observed. Considering the very low value of the corresponding complexation constant (∼0), it seems obvious that the signal corresponding to the complexed dication cannot be observed, because this species is simply not present in the solution.

With the aim of looking further into the results obtained, DFT calculations were carried out on the crown-TTM-TTF molecule in its various states of oxidation, both in metal-free and in complexed forms.

Theoretical Calculations. *Free Crown-TTM-TTF*. The molecular structure of crown-TTM-TTF was fully optimized using the B3P86 functional and the 6-31G** basis set. Owing to the flexibility of the polyether chain, calculations lead to a number of close-energy structures that mainly differ in the conformation of the crown subunit. Figure 3a displays two different views of the minimum-energy structure afforded by the calculations. The structure presents a conformation that strongly resembles that observed in the solid state from X-ray crystallography.[6] The

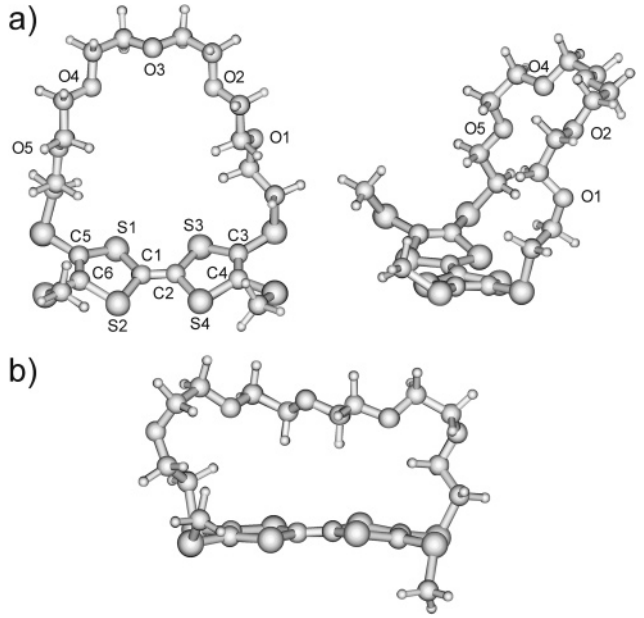

Figure 3. (a) Two different views of the lowest energy molecular conformation calculated for crown-TTM-TTF at the B3P86/6-31G** level. Atomic numbering corresponds to that used in ref 6. (b) A higher energy theoretical structure.

TTF moiety is folded in a boatlike form due to the bending of the dithiolylidene rings along the S···S axes. The average bending angle calculated (20.4°) is larger than that observed in the crystal (5.1°). The polyether chain is positioned upward and shows an orientation of the oxygen lone pairs toward the center of the cavity that is appropriate for complexation purposes. The dimensions predicted for the cavity (7.8 × 8.8 Å) are similar to those observed in the crystal (7.8 × 8.4 Å).[19] Figure 3b presents a theoretical structure in which the TTF moiety is more planar and the polyether chain is less expanded. This structure is calculated 1.53 kcal mol^{-1} higher in energy and shows a conformation less appropriate for metal coordination. Two symmetrized C_s structures showing conformations similar to that depicted in Figure 3a were also generated and optimized, but they were found to be 1.93 and 2.37 kcal mol^{-1} higher in energy. The results presented below therefore correspond to those obtained for the lowest energy structure depicted in Figure 3a.

Figure 4 displays the atomic orbital composition calculated for the highest occupied molecular orbital (HOMO) of crown-TTM-TTF. The electronic density in the HOMO is mainly located over the TTF moiety with small contributions of the thiomethyl sulfurs. This topology suggests that oxidation will mainly affect the structure of the TTF moiety. This is exactly what was obtained when the molecular structures of the cation and dication of crown-TTM-TTF were theoretically optimized. As depicted in Figure 5, the TTF moiety, including the SCH_3 groups, becomes fully planar for the cation, while the polyether chain remains almost unaffected (see Figures 3a and 5). For the dication, the crown ether preserves its conformation but folds down due to the twisting of the SCH_2 units that tend to be coplanar with the TTF moiety. These structural changes are similar to those previously obtained for the TTM-TTF molecule upon oxidation.[11] Neutral TTM-TTF presents a boatlike C_{2v} structure with the four methyl groups pointing upward, while the dication exhibits a planar D_{2h} structure in which the four SCH_3 groups lie within the TTF plane.

Figure 6 summarizes the bond lengths and net atomic charges calculated for the TTM-TTF environment in the different oxidation states of crown-TTM-TTF. Atomic charges were

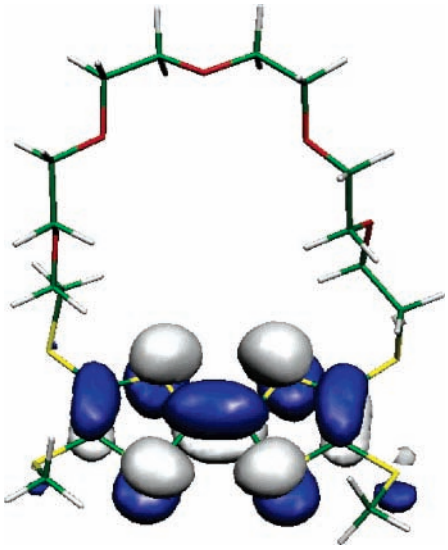

Figure 4. Isodensity representation of the HOMO of crown-TTM-TTF.

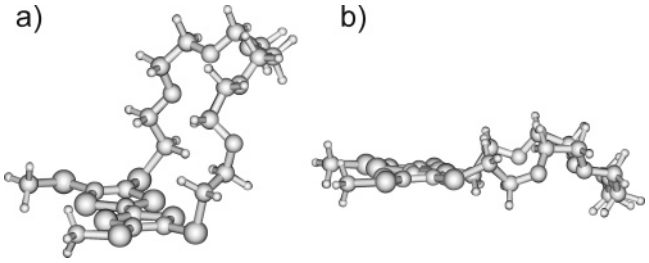

Figure 5. B3P86/6-31G**-optimized structures of the cation (a) and dication (b) of crown-TTM-TTF.

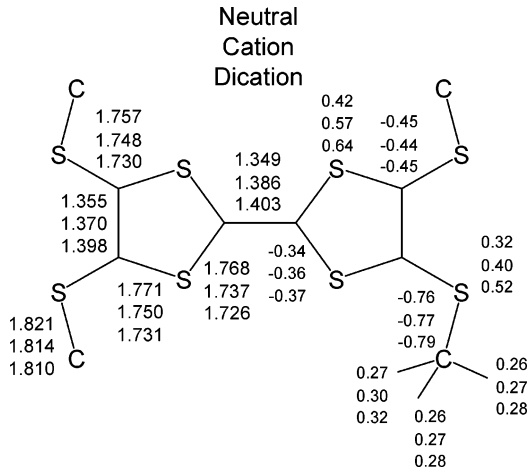

Figure 6. Optimized bond lengths (Å) and NPA net atomic charges (e) calculated for crown-TTM-TTF in its neutral, cation, and dication states.

obtained by using the natural population analysis (NPA) algorithm.[20] For the sake of simplicity, data in Figure 6 are averaged over bonds/atoms that are chemically equivalent in TTM-TTF. In passing from the neutral crown ether to the dication, the central C1−C2 bond lengthens from 1.349 to 1.403 Å, the lateral C3−C4 and C5−C6 bonds elongate from 1.355 to 1.398 Å, and the S−C bonds involving the TTF core shorten by 0.03−0.04 Å. These changes are identical to those previously calculated for the TTM-TTF molecule,[11] and confirm that oxidation mainly affects the TTF moiety. On average, the bonds forming the polyether chain undergo changes smaller than 0.01 Å and those located far from the TTF core remain mainly

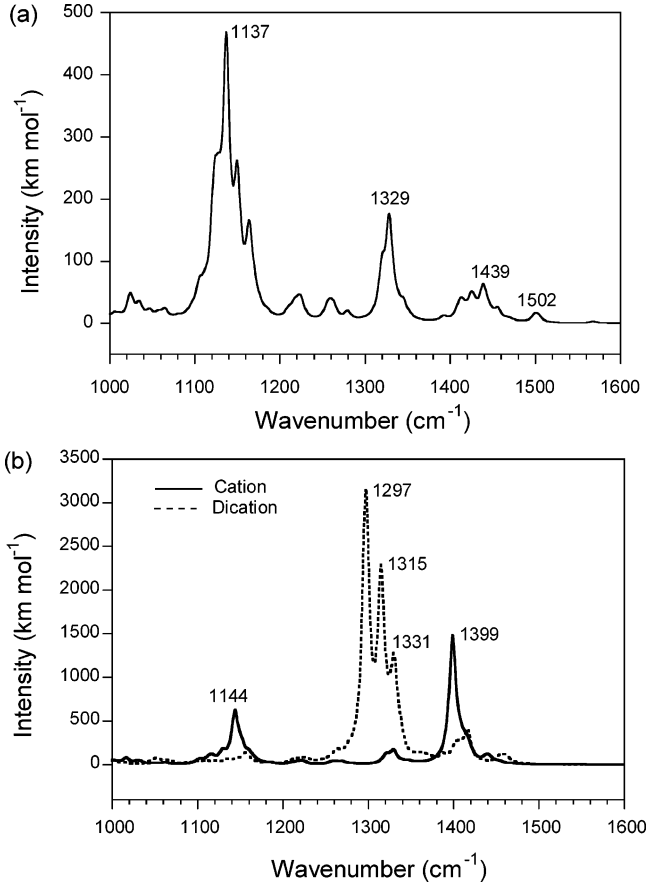

Figure 7. B3P86/6-31G** IR spectra calculated for crown-TTM-TTF in its (a) neutral and (b) cation and dication states.

unaffected. The net atomic charges calculated for crown-TTM-TTF support this result since 0.95 e are extracted from the TTF environment in the radical cation and 1.72 e in the dication.

Figure 7 sketches the IR spectra calculated for crown-TTM-TTF in neutral, cation, and dication states. The spectrum of the neutral species is displayed separately in Figure 7a because of the relatively low intensity of the peaks calculated for this species. The most intense feature corresponds to a multiple-peak structure that originates in a set of normal vibrations associated with the asymmetric stretching motion of the C−O−C ether groups coupled with the rocking of the CH_2 groups. The peak of maximum intensity ($I = 467$ km mol^{-1}) is calculated at 1137 cm^{-1} and mainly involves the motion of the O_1 and O_5 oxygens. The second peak structure centered at 1329 cm^{-1} is due to the umbrella-like motion of the CH_2 and CH_3 groups. The third structure in the 1400−1460 cm^{-1} range mainly results from CH_2 and CH_3 δ deformations. Finally, a low-intensity peak ($I = 17$ km mol^{-1}) is found at 1502 cm^{-1}. This peak arises from the normal modes depicted in Figure 8, which are associated with the in-phase (1500 cm^{-1}) and out-of-phase (1504 cm^{-1}) stretchings of the lateral C3═C4 and C5═C6 double bonds. These vibrations were calculated at almost identical frequencies (1502 and 1506 cm^{-1}, respectively) for the TTM-TTF molecule.[11] A third mode mainly involving the stretching of the central C1═C2 bond is obtained at 1569 cm^{-1} with a negligible intensity ($I = 3$ km mol^{-1}).

The IR band calculated at 1144 cm^{-1} for the crown-TTM-TTF cation (Figure 7b) has the same nature (C−O−C asymmetric stretching) as the structure centered at 1137 cm^{-1} of the neutral system. The upshift of 7 cm^{-1} of the maximum intensity peak is due to a greater participation in the associated normal

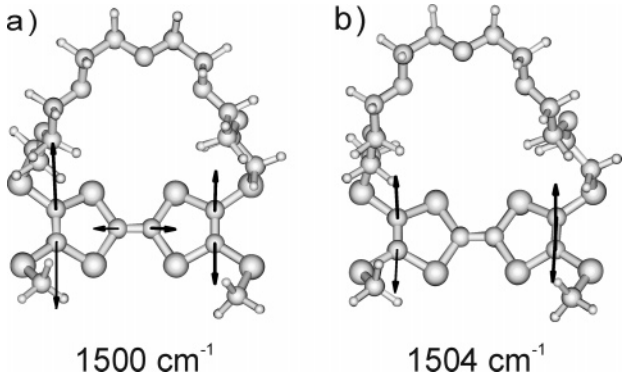

Figure 8. B3P86/6-31G** eigenvectors associated with the in-phase (a) and out-of-phase (b) stretchings of the C3═C4 and C5═C6 bonds calculated for neutral crown-TTM-TTF.

vibration of the C−O_1−C group, which is surrounded by shorter C−C bonds. The most intense feature in the spectrum of the cation is calculated at 1399 cm^{-1} ($I = 1473$ km mol^{-1}) and corresponds to the out-of-phase ν(C═C) vibration sketched in Figure 8b. Oxidation to the cation therefore causes a downshift of 105 cm^{-1} (from 1504 to 1399 cm^{-1}) for that vibration and produces a huge increase of its intensity. This value is comparable to that obtained for TTM-TTF, for which the vibration shifts from 1506 cm^{-1} in the neutral system to 1393 cm^{-1} in the cation. In the crown-TTM-TTF cation, the in-phase ν(C═C) vibration depicted in Figure 8a mixes with the δ deformations of the CH_2 and CH_3 groups and appears as a shoulder on the high-energy side of the 1399 cm^{-1} peak and as a small peak at 1441 cm^{-1}.

The IR spectrum calculated for crown-TTM-TTF^{2+} presents a very intense band structured in three peaks at 1297, 1315, and 1331 cm^{-1}. The most intense peak ($I = 3137$ km mol^{-1}) is due, as for the cation, to the out-of-phase ν(C═C) vibration of the TTF moiety (Figure 8b). The other two peaks result from different vibrations coupling the in-phase ν(C═C) stretching depicted in Figure 8a with the umbrella motions of the CH_2 and CH_3 groups. The lower intensity band around 1420 cm^{-1} results from the δ deformations of the CH_2 and CH_3 groups.

The most relevant changes calculated upon oxidation in the 1000−1600 cm^{-1} region of the IR spectrum of crown-TTM-TTF are therefore those associated with the asymmetric stretching of the lateral C3═C4 and C5═C6 bonds of the TTF unit. As oxidation takes place, this vibration undergoes a frequency downshift (neutral, 1504 cm^{-1}; cation, 1399 cm^{-1}; dication, 1297 cm^{-1}) and an intensity increase (neutral, 8 km mol^{-1}; cation, 1437 km mol^{-1}; dication, 2995 km mol^{-1}). The frequency downshift is due to the lengthening of the C3═C4 and C5═C6 bonds which change from 1.355 Å in the neutral molecule to 1.398 Å in the dication (Figure 6). The intensity increase is due to the electrical dipolar moment induced by the vibrational motion that is expected to augment with the oxidation state due to the increase in the atomic charges (Figure 6). For the dication, two additional intense peaks merge at 1315 and 1331 cm^{-1} due to the in-phase stretching of the C−C bonds of the TTF unit. It should be noted that the same trends and almost identical frequencies were obtained for the optimized C_s structures for which the IR spectra were also calculated.

To make easy the comparison with the experimental results (Figure 2 and Table 1), the IR spectrum calculated for neutral crown-TTM-TTF was subtracted from the spectra obtained for the cation and dication, and the resulting difference spectra are displayed in Figure 9. Calculations predict a negative peak structure centered around 1137 cm^{-1} in the difference spectra

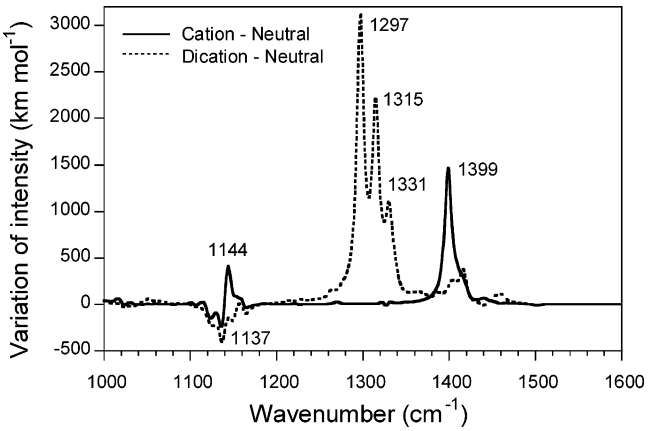

Figure 9. B3P86/6-31G** IR difference spectra calculated for crown-TTM-TTF in its different oxidation states.

of the cation and dication due to the disappearance of the neutral species. This peak can be correlated with the negative band observed experimentally around 1103 cm^{-1} and is due to the asymmetric stretching of the C−O−C groups as assigned above.

The theoretical difference spectrum of the cation presents two positive peaks at 1144 and 1399 cm^{-1}. The former peak results from the shift of the C−O−C stretching in passing to the cation and is not detected in the experimental spectrum. Indeed, the appearance of this peak depends on the conformation of the polyether chain, and it is not predicted when the more symmetric C_s structures are used in the calculation of the IR spectra. The intense peak at 1399 cm^{-1} matches perfectly the experimental peak observed at 1398 cm^{-1}, which is thus assigned to the out-of-phase stretching of the C3═C4 and C5═C6 bonds. The experimental peak at 1322 cm^{-1} was assigned to the umbrella-like vibrational motion of the CH_3 groups in TTM-TTF (1319 cm^{-1}).[11] For the crown-TTM-TTF cation, these vibrations are calculated around 1320−1330 cm^{-1} and remain almost unaffected in passing from the neutral system to the cation. Therefore, no prominent peak is obtained in the theoretical difference spectrum.

For the dication, the intense three-peak structure calculated at 1297, 1315, and 1331 cm^{-1} accounts for the experimental band structured in three peaks observed at 1295, 1315, and 1332 cm^{-1} (see Table 1). As discussed above, these peaks correspond to C═C stretchings of the TTF moiety that shift down upon oxidation. The δ deformations of the CH_2 and CH_3 groups calculated in the 1400−1420 cm^{-1} range are not detected in the experimental spectrum. This was also the case for TTM-TTF^{2+}.[11]

We have therefore shown that IR spectroelectrochemistry can be safely used to monitor the various redox steps in the oxidation process of crown-TTM-TTF. Although the experimental peaks have a very low intensity, the maximum variation of absorbance is lower than 0.02, and the technique clearly identifies the distinctive peaks that characterize each species. The neutral species is recognized by the negative peak around 1100 cm^{-1}. The signature of the cation is the intense band at 1398 cm^{-1} associated with the stretching of the lateral C═C bonds of the TTF moiety. This band can also be used to identify the dication because it downshifts by approximately 100 cm^{-1} and forms a well-resolved, three-peak intense structure.

Barium Complex of Crown-TTM-TTF. The molecular structure of the complex formed by crown-TTM-TTF and Ba^{2+} was fully optimized starting from the conformation depicted in Figure 3a and from the more symmetric C_s conformations after insertion of a barium cation into the middle of the polyether

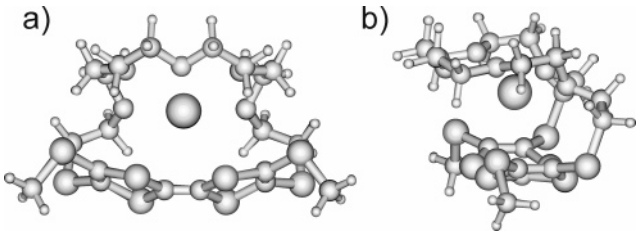

Figure 10. B3P86/6-31G**-optimized, lowest energy structure of the Ba^{2+}−crown-TTM-TTF complex (C_s symmetry): (a) frontal view; (b) lateral view.

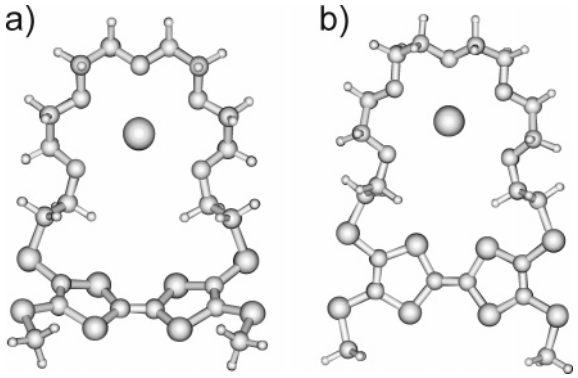

Figure 11. B3P86/6-31G**-optimized structures of the radical cation (a) and dication (b) of the Ba^{2+}−crown-TTM-TTF complex (C_s symmetry).

chain. The most stable structure now corresponds to the C_s conformation displayed in Figure 10, which is calculated to be 3.30 kcal mol^{-1} lower in energy than that resulting from the asymmetric conformation of Figure 3a. Compared to that of the metal-free system, the polyether chain folds down over the TTF moiety, forming a cavity in which the Ba^{2+} cation is embedded at almost equal distances from the five oxygen atoms (2.76−2.87 Å). The TTF moiety preserves its boat conformation, showing an average bending angle of 18.5° along the S···S axes. The conformation predicted for the complex is, however, significantly different from that observed in the crystal, in which the polyether chain is more extended.[6] The difference comes from the fact that the coordination of Ba^{2+} in the solid is ensured by the five oxygen atoms forming the polyether chain, and also by solvent molecules (H_2O/CD_3CN) and counterions ($CF_3SO_3^-$), giving rise to a 10-fold coordination sphere. Calculations lead to a more compact structure, in which the barium cation is more effectively surrounded by the crown ether (Figure 10), because only the coordination by the polyether oxygens is taken into account. The calculation of the equilibrium structure of the complex including the counterions (ClO_4^-) and the solvent molecules (CH_3CN/CH_2Cl_2) involved in the spectroelectrochemistry experiment is precluded by the size of the system and because the actual coordination of the Ba^{2+} cation in the solution is unknown. Despite these limitations, the Ba···O distances predicted theoretically (2.76−2.87 Å) are rather close to those observed by X-ray diffraction (2.88−2.92 Å).[6]

The structures of the radical cation and dication were calculated starting from the optimized structure of the neutral complex and are depicted in Figure 11. As oxidation takes place, the polyether chain spreads out and gives rise to more extended structures, in which the barium cation moves away from the TTF core. The distance from the Ba^{2+} ion to the S1 and S3 atoms changes from 3.87 Å in the neutral system to 6.30 Å in the radical cation and 5.98 Å in the dication. In contrast, the average distance between the Ba^{2+} ion and the oxygen atoms

of the polyether chain remains almost constant (neutral, 2.82 Å; cation, 2.81 Å; dication, 2.86 Å).

Calculations clearly show that oxidation mainly affects the TTF moiety. In passing to the dication, the bond lengths undergo changes similar to those collected in Figure 6 for the metal-free molecule. The central C1═C2 bond lengthens from 1.357 to 1.406 Å, the lateral C3═C4 and C5═C6 bonds increase from 1.354 to 1.405 Å, and the C−S bonds shorten by 0.03−0.06 Å. The NPA net atomic charges calculated for the different species indicate that the electrons are mainly removed from the TTF environment. The total charge extracted from this environment is 0.95 e for the radical cation and 1.94 e for the dication. This latter value is higher than that obtained for the noncomplexed system (1.72 e) and indicates a higher accumulation of the positive charge on the TTF core due to the repulsive electrostatic effect of the Ba^{2+} cation.

The stability of the Ba^{2+}−crown-TTM-TTF complex was estimated as the difference between the total energies of the noncomplexed and complexed systems. The binding energy calculated at the B3P86/6-31G** level for the Ba^{2+}−crown-TTM-TTF complex is 162.30 kcal mol^{-1}, thus supporting the complexation ability of neutral crown-TTM-TTF. Upon oxidation, the binding energy decreases to 53.14 kcal mol^{-1} for the cation and becomes negative (−38.18 kcal mol^{-1}) for the dication. These energies suggest that the Ba^{2+} ion remains complexed when the crown-TTM-TTF ligand is oxidized to the radical cation but is expelled when the dication is formed. Calculations therefore reinforce the experimental evidence indicating that the formation of the dication implies the expulsion of barium from the cage of the crown ether.

The IR spectrum of the complexed system was thus calculated only for the neutral and radical cation states of the crown ether. The comparison of the theoretical spectra with the experimental spectra is not straightforward because the former are obtained for isolated systems and do not include the solvent molecules and the counterions that surround the Ba^{2+} ion in solution. Despite this limitation, clear correlations between the theoretical results and the experimental data can be established. For the neutral ligand, the complexation with Ba^{2+} generates a theoretical displacement toward lower frequencies (from 1137 to 1094 cm^{-1}) of the negative peak appearing in the difference spectrum. This displacement correlates with the downshift observed in the experimental spectra from 1103 to 1079 cm^{-1} (see Tables 1 and 2). As discussed above, the peak was due to the asymmetric stretching motion of the C−O−C ether groups and involves the deformation of the polyetheroxide chain. The peak shifts down because the incorporation of the Ba^{2+} cation determines an elongation of the C−O bonds from ∼1.41 Å in the metal-free system to ∼1.43−1.44 Å in the complexed crown ether. These results therefore support that the experimental peak observed at 1079 cm^{-1} is the signature of the complexed state of neutral crown-TTM-TTF.

As for the radical cation, calculations predict that the complexed system shows a very intense peak (I = 1574 km mol^{-1}) at 1371 cm^{-1}. The peak has the same nature (the out-of-phase ν(C═C) stretching sketched in Figure 8b) as the intense peak calculated at 1399 cm^{-1} for the metal-free system (see Figure 7b), and it shifts down due the lengthening of the C3═C4 and C5═C6 bonds (∼0.01 Å) caused by Ba^{2+} complexation. The frequency predicted for the peak lies in one of the zones where the solvent presents a strong absorption (1375 cm^{-1}) and the peak is not experimentally observed because it is probably masked by the solvent. The weak feature observed at 1345 cm^{-1} in the experimental spectra of the cation (Table 2) can be attributed to the normal modes associated with the umbrella-like vibrations of the CH_2 and CH_3 groups calculated around 1330 cm^{-1}. These vibrations increase their intensity with complexation and give rise to a small feature (I = 154 km mol^{-1}) in the difference spectrum. This intensity increase was not obtained for the metal-free system, and the spectral feature observed at 1345 cm^{-1} can be taken as a signature of the complexation of the crown-TTM-TTF radical cation.

The theoretical difference spectrum calculated for the complexed radical cation shows more intense features in the spectral region 970−1070 cm^{-1}. These features correspond to vibrational modes involving the oxygen atoms of the polyether chain and are more sensitive to the presence of the Ba^{2+} cation in the cage. Unfortunately, they are experimentally obscured by the absorption of the solvent and by the optical window. Indeed, the CaF_2 window used in the experiment cuts off at 1111 cm^{-1}; i.e., the energy of the beam decreases considerably between 1100 and 1000 cm^{-1}, and no more signal can be detected below 1000 cm^{-1}. Therefore, to be able to reach the spectral range between 900 and 1000 cm^{-1}, one could use IRTRAN (zinc selenide, ZnSe, 20000−454 cm^{-1}). However, in our experimental configuration (incidence of the beam 30° relative to the normal), the specular reflection is very intense because of the high refractive index of ZnSe (n = 2.4), which will strongly degrade the signal-to-noise ratio. In view of this, the observation of the zone below 1000 cm^{-1} seems to be quite difficult to obtain.

4. Conclusion

Crown ethers are cyclic polyethers that have the property of complexing metal cations. By grafting electroactive moieties onto such molecules and taking care of achieving an optimal coupling between the two components of the assembly, it is possible to control electrochemically the complexation/decomplexation process. In this family of new molecules, a crown-TTF has been studied. It keeps the electrochemical properties of TTF and has a good affinity toward the barium metal cation. A previous electrochemical study had shown that the formation of the radical cation involves a partial decomplexation, whereas the formation of the dication causes the full expulsion of the cation from the crown-TTF cage.

An in situ, real time FTIR spectroelectrochemistry study has been undertaken to obtain the spectroscopic signature of this expulsion phenomenon. DFT modeling has been carried out on both the free and the complexed molecules in their various oxidation states. The theoretical IR spectra have allowed a full interpretation of the changes observed upon oxidation in the experimental difference spectroelectrogram, showing that IR signals can be used as structural signatures to identify the different oxidation states. The results obtained and presented in this work ascertain the fact that the neutral crown-TTF derivative is able to complex barium: the presence of the metal cation inside the cage induces a 24 cm^{-1} downshift of the corresponding absorbance peak. The spectroscopic signature of the radical cation of the complexed crown-TTF was more difficult to identify, but the results obtained were enforced by DFT calculations: a new peak is formed at 1345 cm^{-1}. Due to the fact that the amount of complexed species is lower than that of the free species, this peak could only be detected for an addition of 16 equiv of barium. Additionally, both experimental and theoretical studies evidenced that the complexed form of the dication does not exist. In view of this, it is possible to confirm that the complexation/decomplexation of the crown-TTF can be triggered electrochemically.

Acknowledgment. The research at the University of València was supported by the Ministerio de Educacion, Cultura y Deporte (MECD) of Spain, and European FEDER funds through Project BQU2003-05111. Financial support was also provided by the Generalitat Valenciana (Grant OCYT-GRUPOS03/173).

References and Notes

(1) (a) Cram, D. J. *Angew. Chem., Int. Ed. Engl.* **1988**, *27*, 1009. (b) Pedersen, C. J. *Angew. Chem., Int. Ed. Engl.* **1988**, *27*, 1021. (c) Lehn, J. M. *Angew. Chem., Int. Ed. Engl.* **1988**, *27*, 90. (d) Dietrich, B.; Viout, P.; Lehn, J. M. *Aspect de la chimie des composés macrocycliques*; InterEditions/ Ed. du CNRS, 1991. (e) Lehn, J. M. *La chimie supramoléculaire*; Deboeck Université, 1997. (f) Gokel, G. W.; Murillo, O.; Bradshaw, J. S.; Izatt, R. W.; Borunov, A. V.; Zhu, C. Y.; Hathaway, J. K.; Schall, O. F.; Dietrich, B.; Maverick, E.; Cram, D. J.; Telford, J.; Raymond, K. N. *Compr. Supramol. Chem.* **1995**, *1*, 1−6.

(2) (a) Hurtley, W. R.; Smiles, S. *J. Chem. Soc.* **1926**, 1821 and 2263. (b) Wudl, F.; Wobschall, D.; Hufnagel, E. J. *J. Am. Chem. Soc.* **1972**, *94*, 670. (c) Ferraris, J.; Cowan, D. O.; Walatka, V.; Perlstein, J. H. *J. Am. Chem. Soc.* **1973**, *95*, 948. (d) Coleman, L. B.; Cohen, M. J.; Sandman, D. J.; Yamaguchi, F. G.; Garito, A. F.; Heeger, A. G. *Solid State Commun.* **1973**, *12*, 1125. (e) Jérome, D.; Mazaud, A.; Ribault, M.; Bechgaard, K. *J. Phys. Lett.* **1980**, *41*, 95. (f) Bechgaard, K.; Jacobsen, C. S.; Mortensen, K.; Pedersen, H. J.; Thorup, N. *Solid State Commun.* **1980**, *33*, 1119. (g) Parkin, S. S. P.; Engler, E. M.; Schumaker, R. R.; Lagier, R.; Lee, V. Y.; Scott, J. C.; Greene, R. L. *Phys. Rev. Lett.* **1983**, *50*, 270. (h) Bryce, M. R. *Chem. Soc. Rev.* **1991**, *20*, 355. (i) Adam, M.; Müllen, K. *Adv. Mater.* **1994**, *6*, 439. (j) Khodorkovsky, V.; Becker, J. Y. Molecular design of organic conductors. In *Organic Conductors*; Farges, J. P., Ed.; Marcel Dekker, Inc.: New York, 1994; p 75. (k) Bryce, M. R. *J. Mater. Chem.* **1995**, *5*, 1481.

(3) (a) Otsubo, T.; Ogura, F. *Bull. Chem. Soc. Jpn.* **1985**, *58*, 1343. (b) Steimecke, G.; Sieler, H. J.; Kirmse, R.; Hoyer, E. *Sulfur Phosphorus Chem.* **1979**, *7*, 49. (c) Hansen, T. K.; Joergensen, T.; Stein, P. C.; Becher, J. *J. Org. Chem.* **1992**, *57*, 6403. (d) Hansen, T. K.; Stein, P. C. *Synth. Met.* **1993**, *55*, 1972. (e) Dieing, R.; Morisson, V.; Moore, A. J.; Goldenberg, L. M.; Bryce, M. R.; Raoul, J. M.; Petty, M. C.; Garín, J.; Saviron, M.; Lednev, I. K.; Hester, R. E.; Moore, J. N. *J. Chem. Soc., Perkin Trans. 2* **1996**, 1587. (f) Joergensen, T.; Girmay, B.; Hansen, T. K.; Becher, J.; Underhill, A. E.; Hursthouse, M. B.; Harman, M. E.; Kilburn, J. D. *J. Chem. Soc., Perkin Trans. 1* **1992**, 2907. (g) Gemmell, C.; Janairo, G. C.; Kilburn, J. D.; Ueck, H.; Underhill, A. E. *J. Chem. Soc., Perkin Trans. 1* **1994**, 2715.

(4) (a) Jørgensen, T.; Hansen, T. K.; Becher, J. *Chem. Soc. Rev.* **1994**, *23*, 41. (b) Bryce, M. R. *Adv. Mater.* **1999**, *11*, 11. (c) Bryce, M. R. *J. Mater. Chem.* **2000**, *10*, 589. (d) Nielsen, M. B.; Lomholt, C.; Becher, J. *Chem. Soc. Rev.* **2000**, *29*, 153. (e) Segura, J. L.; Martín, N. *Angew. Chem., Int. Ed.* **2001**, *40*, 1372.

(5) (a) Joergensen, T.; Girmay, B.; Hansen, T. K.; Becher, J.; Underhill, A. E.; Hursthouse, M. B.; Harman, M. E.; Kilburn, J. D. *J. Chem Soc., Perkin Trans. 1* **1992**, 2907. (b) Gemmell, C.; Janario, G. C.; Kilburn, J. D.; Ueck, H.; Underhill, A. E. *J. Chem. Soc., Perkin Trans. 1* **1994**, 2715. (c) Wagner, M.; Madsen, D.; Markussen, J.; Larsen, S.; Schaumburg, K.; Lubert, K. H.; Becher, J.; Olk, R. M. *J. Chem. Soc., Perkin Trans. 1* **1996**, 1995. (d) Wagner, M.; Pink, M.; Olk, R. M. *Phosphorus, Sulfur Silicon* **1996**, *116*, 283. (e) Lubert, K. H.; Wagner, M.; Olk, R. M. *Anal. Chim. Acta* **1996**, *336*, 77. (f) Gasiorowski, R.; Jorgensen, T.; Moller, J.; Hansen, T. K.; Pietraszkiewicz, M.; Becher, J. *Adv. Mater.* **1992**, *9*, 568. (g) Hansen, T. K.; Joergensen, T.; Jensen, F.; Thygesen, P. H.; Christiansen, K.; Hurthouse, M. B.; Harman, M. E.; Malik, M. A.; Girmay, B.; Underhill, A. E.; Begtrup, M.; Kilburn, J. D.; Belmore, K.; Roespstorff, P.; Becher, J. *J. Org. Chem.* **1993**, *58*, 1359.

(6) (a) Le Derf, F.; Mazari, M.; Mercier, N.; Levillain, E.; Richomme, P.; Becher, J.; Garín, J.; Orduna, J.; Gorgues, A.; Sallé, M. *Inorg. Chem.* **1999**, *38*, 6096. (b) Le Derf, F.; Mazari, M.; Mercier, N.; Levillain, E.; Trippé, G.; Riou, A.; Richomme, P.; Becher, J.; Garín, J.; Orduna, J.; Gallego-Planas, N.; Gorgues, A.; Sallé, M. *Chem. Eur. J.* **2001**, *7*, 447.

(7) Hartmann, H.; Scheiring, T.; Fiedler, J.; Kaim, W. *J. Organomet. Chem.* **2000**, *604*, 267.

(8) Gaillard, F.; Levillain, E. *J. Electroanal. Chem.* **1995**, *398*, 77.

(9) Bellec, V.; DeBacker, M. G.; Levillain, E.; Sauvage, F. X.; Wartelle, C. *Electrochem. Commun.* **2001**, *3*, 483.

(10) Dias, M.; Perrin, L.; Hudhomme, P.; Levillain, E.; Şahin, Y.; Sauvage, F. X.; Wartelle, C. *Electrochem. Commun.* **2004**, *6*, 325.

(11) Wartelle, C.; Viruela, R.; Viruela, P.; Sauvage, F. X.; Sallé, M.; Ortí, E.; Levillain, E.; Le Derf, F. *Phys. Chem. Chem. Phys.* **2003**, *5*, 4672.

(12) Khodorkovsky, V.; Shapiro, L.; Krief, P.; Shames, A.; Mabon, G.; Gorgues, A.; Giffard, M. *Chem. Commun.* **2001**, 2736.

(13) Frisch, M. J.; Trucks, G. W.; Schlegel, H. B.; Scuseria, G. E.; Robb, M. A.; Cheeseman, J. R.; Montgomery, J. A.; Vreven, T.; Kudin, K. N.; Burant, J. C.; Millam, J. M.; Iyengar, S. S.; Tomasi, J.; Barone, V.; Mennucci, B.; Cossi, M.; Scalmani, G.; Rega, N.; Petersson, G. A.; Nakatsuji, H.; Hada, M.; Ehara, M.; Toyota, K.; Fukuda, R.; Hasegawa, J.; Ishida, M.; Nakajima, T.; Honda, Y.; Kitao, O.; Nakai, H.; Klene, M.; Li, X.; Knox, J. E.; Hratchian, H. P.; Cross, J. B.; Adamo, C.; Jaramillo, J.; Gomperts, R.; Stratmann, R. E.; Yazyev, O.; Austin, A. J.; Cammi, R.; Pomelli, C.; Ochterski, J. W.; Ayala, P. Y.; Morokuma, K.; Voth, G. A.; Salvador, P.; Dannenberg, J. J.; Zakrzewski, V. G.; Dapprich, S.; Daniels, A. D.; Strain, M. C.; Farkas, O.; Malick, D. K.; Rabuck, A. D.; Raghavachari, K.; Foresman, J. B.; Ortiz, J. V.; Cui, Q.; Baboul, A. G.; Clifford, S.; Cioslowski, J.; Stefanov, B. B.; Liu, G.; Liashenko, A.; Piskorz, P.; Komaromi, I.; Martin, R. L.; Fox, D. J.; Keith, T.; Al-Laham, M. A.; Peng, C. Y.; Nanayakkara, A.; Challacombe, M.; Gill, P. M. W.; Johnson, B.; Chen, W.; Wong, M. W.; Gonzalez, C.; Pople, J. A. *GAUSSIAN 03*; Gaussian, Inc., Pittsburgh, PA, 2003.

(14) Perdew, J. P. *Phys. Rev. B* **1986**, *33*, 822.

(15) Francl, M. M.; Pietro, W. J.; Hehre, W. J.; Binkley, J. S.; Gordon, M. S.; Defrees, D. J.; Pople, J. A. *J. Chem. Phys.* **1982**, *77*, 3654.

(16) (a) Viruela, P. M.; Viruela, R.; Ortí, E.; Brédas, J. L. *J. Am. Chem. Soc.* **1997**, *119*, 1360. (b) Liu, R.; Zhou, X.; Kasmai, H. *Spectrochim. Acta, A* **1997**, *53*, 1241. (c) Altmann, J. A.; Handy, N. C.; Ingamells, O. C. *Mol. Phys.* **1997**, *92*, 339. (d) Casado, J.; Miller, L. L.; Mann, K. R.; Pappenfus, T. M.; Kanemitsu, Y.; Ortí, E.; Viruela, P. M.; Pou-Amérigo, R.; Hernández, V.; López-Navarrete, J. *J. Phys. Chem. B* **2002**, *106*, 3872.

(17) Hay, P. J.; Wadt, W. R. *J. Chem. Phys.* **1985**, *82*, 270, 284, 299.

(18) Scott, A. P.; Radom, L. *J. Phys. Chem.* **1996**, *100*, 16502.

(19) The cavity size is defined by [d(O1−O5) x $^1/_2$[d(O3−S1) + d(O3−S3)]]. Atomic numbering is given in Figure 3a and corresponds to the crystallographic numbering used in ref 6.

(20) Reed, A. E.; Curtiss, L. A.; Weinhold, F. *Chem. Rev.* **1988**, *88*, 899.